Sustainability **2015**, *7*, 11401-11417; doi:10.3390/su70911401

OPEN ACCESS

sustainability

ISSN 2071-1050

www.mdpi.com/journal/sustainability

Article

Temperature Vegetation Dryness Index Estimation of Soil Moisture under Different Tree Species

Shulin Chen [1,2], Zuomin Wen [1,*], Hong Jiang [2], Qingjian Zhao [1], Xiuying Zhang [2] and Yan Chen [1]

1 College of Economics and Management, Nanjing Forestry University, Nanjing 210000, China; E-Mails: chenshulin0923@163.com (S.C.); zhao5190@126.com (Q.Z.); sanchen007@163.com (Y.C.)

2 International Institute for Earth System Science, Nanjing University, Nanjing 210000, China; E-Mails: jianghong@nju.edu.cn (H.J.); lzhxy77@163.com (X.Z.)

* Author to whom correspondence should be addressed; E-Mail: zmwen@njfu.edu.cn; Tel.: +86-25-8542-7088; Fax: +86-25-8542-7377.

Academic Editor: Eric Vaz

Received: 1 July 2015 / Accepted: 12 August 2015 / Published: 25 August 2015

Abstract: The Laoshan forest is the largest forest in Nanjing, and it plays an important role in water resource management in Nanjing. The objectives of this study are to determine if the temperature vegetation dryness index (TVDI) is suitable to estimate the soil moisture and if soil moisture is significantly affected by tree species in the Laoshan forest. This paper calculated the spatial distribution of TVDI using LANDSAT-5 TM data. Sixty-two observation points of *in situ* soil moisture measurements were selected to validate the effectiveness of the TVDI as an index for assessing soil moisture in the Laoshan forest. With the aid of the three different temporal patterns, which are 10 January 2011, 18 May 2011 and 23 September 2011, this paper used the TVDI to investigate the differences of soil moisture under four kinds of mono-species forests and two kinds of mixed forests. The results showed that there is a strong and significant negative correlation between the TVDI and the *in situ* measured soil moisture (R^2 = 0.15–0.8, SE = 0.015–0.041 cm^3/cm^3). This means that the TVDI can reflect the soil moisture status under different tree species in the Laoshan forest. The soil moisture under these six types of land cover from low to high is listed in the following order: *Eucommia ulmoides*, *Quercus acutissima*, broadleaf mixed forest, *Cunninghamia lanceolata*, coniferous and broadleaf mixed forest and *Pinus massoniana*.

Keywords: soil moisture; NDVI; surface temperature; TVDI; tree species

1. Introduction

Soil moisture is a very important variable of the climate system, as it controls numerous processes and feedback loops within the climate system. It is of major relevance for the global water, energy and carbon cycles [1]. Increased climate change is altering the global water cycle and affecting the amount of water available for tree species. Differences in soil water content of tree species are becoming increasingly important to identify with global climate changes [2]. The Laoshan forest is the largest forest in Nanjing. In addition, with the rapid growth of the economy and urban population, the problem of supply and demand for water in Nanjing has become increasingly important over the past several decades [3]. Therefore, knowledge of the state of soil moisture for different tree species over time in the Laoshan forest is essential for a wide range of meteorological and hydrological applications, such as weather and climate prediction, terrestrial carbon cycle simulation, water management and policy planning.

There are many different techniques for *in situ* soil moisture measurement under tree species, such as the gravimetric method, neutron probe, heat dissipation sensor, time domain reflectometry (TDR), frequency domain reflectometry (FDR), *etc*. [4,5]. However, *in situ* soil moisture measurements are cost intensive and require major efforts to be put in place. As a result, only a few *in situ* soil moisture measurement networks are available. In addition, it is often questioned whether the point measurements for regional applications are representative [6,7].

Remote sensing is currently in a strong position to provide meaningful spatial and temporal data for use in soil moisture investigations. Over the past 40 years, substantial research has been carried out to retrieve soil moisture using remotely-sensed observations [8], but little research focused on investigating the differences of soil moisture under different tree species. Therefore, this paper investigates the suitability of remote sensing for estimating the soil moisture of different tree species in the Laoshan forest. In this study, the accuracy of estimated soil water content under different tree species is investigated with the aid of three different temporal patterns.

The normalized difference vegetation index (NDVI) can monitor vegetation status and stress, specifically in relation to water stress, and the forest canopy temperature (T_s) will rise rapidly with water stress [9,10]. The potential for obtaining soil moisture through the relationship between remotely-sensed T_s and NDVI has been investigated by several authors [9–11]. The slope of the T_s/NDVI curve is related to the evapotranspiration rate of the surface and is used to assess soil moisture conditions. Numerous studies focus on the slope of the T_s/NDVI curve for this purpose [12]. The scatter plots of T_s/NDVI space often result in a triangular shape [10,13] or a trapezoidal shape [14,15].

Sandholt *et al*. [10] explored a simplified land surface dryness index, called the temperature vegetation dryness index (TVDI), based on an empirical parameterization of the relationship between T_s and NDVI. Following this, different satellite images have been used to demonstrate the potential of the TVDI for soil moisture estimation, such as the National Oceanic and Atmospheric Administration (NOAA) Advanced Very High Resolution Radiometer (AVHRR) images [10,16], Terra/Aqua Moderate-Resolution Imaging Spectroradiometer (MODIS) images [7,8,17–20] and LANDSAT-5

Thematic Mapper (TM) images [21]. The comparisons with soil moisture *in situ* measurements or model simulations show that the TVDI is feasible for monitoring soil moisture.

The scale effect is one of the very important scientific problems of remote sensing [22], and it can increase uncertainty in soil moisture retrieval. LANDSAT-5 TM images have a higher spatial resolution (30–120 m) than Terra/Aqua MODIS (250–1000 m) images or NOAA-AVHRR (1100 m) images, so this study uses LANDSAT-5 TM images.

There are two objectives of this study: (i) to determine the suitability of TVDI for estimating the soil moisture in the Laoshan forest; and (ii) to determine if soil moisture is significantly affected by tree species. Three different temporal patterns of satellite images, 10 January 2011, 18 May 2011 and 23 September 2011, were selected in this study.

2. Study Area

The Laoshan forest is located in Nanjing Jiangsu Province in East China between 32°02′34″ and 32°09′54″ N latitude and 118°24′33″ and 118°41′15″ E longitude (Figure 1). Its range is 35 km from east to west, and 15 km from south to north. The total area is 7493 ha. There are some water reservoirs in the Laoshan forest, and thematic maps of them were generated from the forest inventory organized by the Jiangsu Provincial Forestry Bureau in 2007.

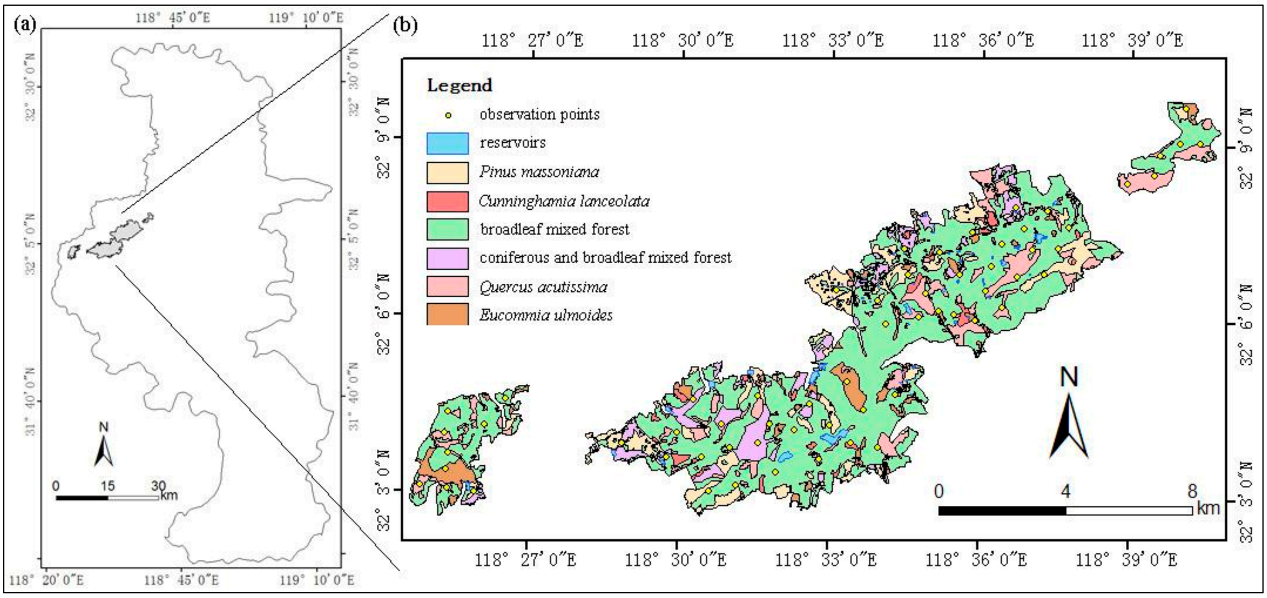

Figure 1. The location of the Laoshan forest in Nanjing. (**a**) The location of the Laoshan forest in Nanjing and (**b**) the types of land cover in the Laoshan forest region. The yellow points in (b) are the sixty-two observation points of *in situ* soil moisture measurements.

There are four kinds of mono-species and two kinds of mixed forests in the Laoshan forest. The tree species of these mono-species forests are *Cunninghamia lanceolata*, *Eucommia ulmoides*, *Quercus acutissima* and *Pinus massoniana*. The two kinds of mixed forests are broadleaf mixed forest and coniferous and broadleaf mixed forest. There are three different types of tree species in the broadleaf mixed forest, and they are *Quercus acutissima*, *Celtis sinensis* and *Sophora japonica*. The coniferous and broadleaf mixed forest mainly consists of the following five different types of tree species, which are *Quercus acutissima*, *Pterocarya stenoptera*, *Celtis sinensis*, *Pinus massoniana* and exotic pine. The areas of each land cover type in the Laoshan forest are presented in Table 1.

Table 1. The areas of each land cover type in the Laoshan forest.

Land Cover Type	Area (units: ha)
broadleaf mixed forest	5364.988
Quercus acutissima	704.342
Pinus massoniana	606.933
coniferous and broadleaf mixed forest	359.664
Eucommia ulmoides	269.748
Cunninghamia lanceolata	187.325

3. Methodology

This study uses a land surface dryness index called TVDI to estimate the soil moisture under different tree species in the Laoshan Forest. Figure 2 presents a flowchart of the soil moisture estimation of different tree species assessment. All steps will be discussed in detail below.

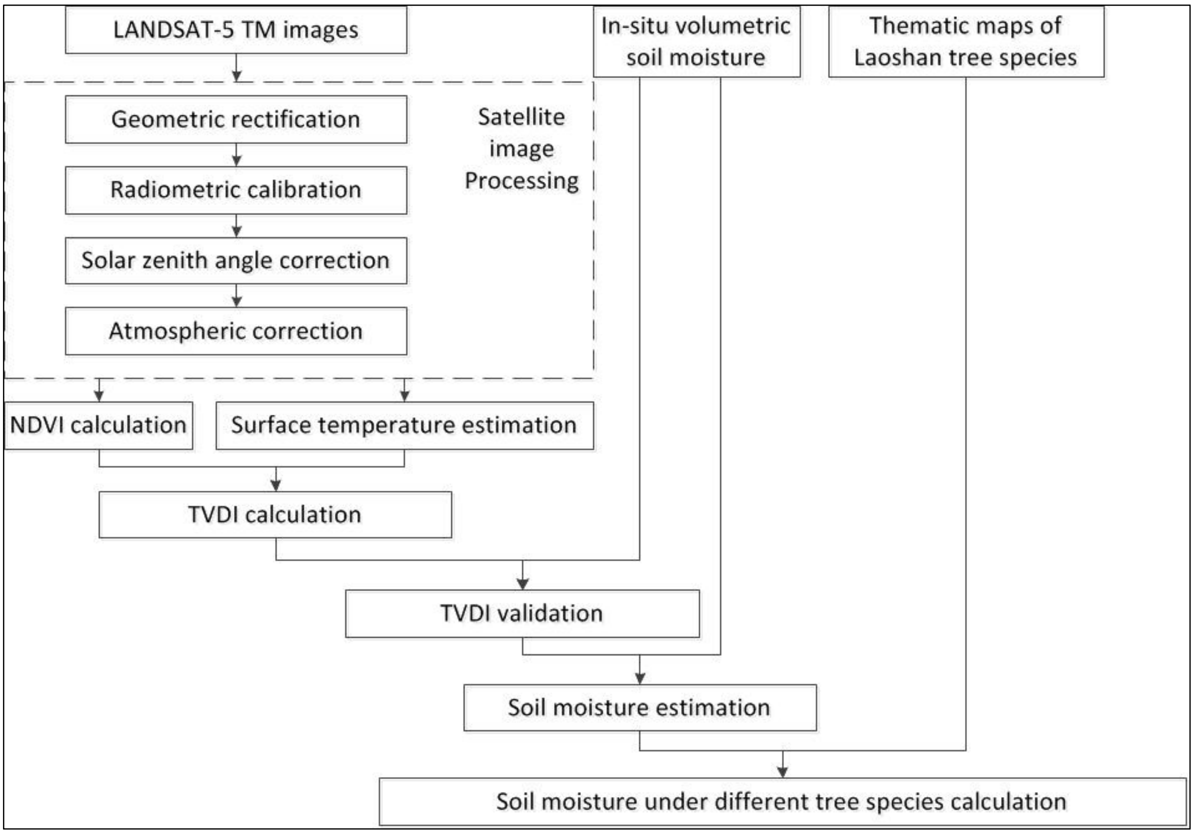

Figure 2. The flowchart of the soil moisture under different tree species' assessment.

3.1. Field Work

In order to carry out the analysis for different vegetation covers and different temporal patterns, sixty-two observation points of *in situ* soil moisture measurements were selected to ensure that each tree species had at least five observation points (see Figure 1). The method of TVDI is based on the feedbacks of soil moisture content to the forest canopy temperature. The soil moisture content within the root zone affects the plants' transpiration. With decreasing soil moisture content, the soil suction increases, the remaining soil moisture becomes less available for uptake by plant roots, the transpiration might thus become reduced and, then, the forest canopy temperature will increase [1]. Previous results showed that in the root zone of the soil profile, the relationships between the TVDI and soil moisture at depths of 0–20 cm of soil samples were closer than other depths [7,17,19,23,24]. Based on these previous results, for this study, volumetric soil samples (the volume of each soil sample is 100 cm^3) were collected 0–15 cm deep. The sample mass and volume were determined before and after oven drying (*i.e.*, generally drying sample in an oven set at 105 degrees Celsius for 12 h) to determine gravimetric water content, bulk density and, hence, volumetric water content.

3.2. Satellite Image Processing

In this study, image rectification, including geometric rectification, radiometric calibration, solar zenith angle correction and atmospheric correction, has been accomplished using ENVI™ image processing software (Version 4.7). Radiometric calibration of Landsat-5 TM is based on the analysis of Chander *et al*. [25]. Atmospheric correction of Landsat-5 TM is accomplished using the ENVI FLAASH (Fast Line-of-sight Atmospheric Analysis of Hypercubes, FLAASH) model which is based on the MODTRAN4 RT model [26].

3.3. Calculation of Normalized Difference Vegetation Index

NDVI is the observed normalized difference vegetation index, and it can be defined as:

$$\mathrm{NDVI} = (\rho_{\mathrm{nir}} - \rho_{\mathrm{red}})/(\rho_{\mathrm{nir}} + \rho_{\mathrm{red}}) \tag{1}$$

where ρ_{nir} is the near-infrared band reflectance and ρ_{red} is the red band reflectance. In this study, NDVI was calculated using LANDSAT-5 TM Band 3 (the red band) reflectance and LANDSAT-5 TM Band 4 (the near-infrared band) reflectance.

3.4. Retrieval of Surface Temperature (T_s)

Qin *et al*. [27] developed a mono-window algorithm for retrieving surface temperature from LANDSAT-5 TM Band 6 data. Many researchers have validated the algorithm and have shown that the algorithm provides an RMSD value of 0.9–1.1 K [28–30]. Thus, this study uses this algorithm to obtain the T_s. The MODIS land surface temperature products (MOD11A1, Version 5) were used to validate the T_s. These data have been downloaded from the Land Processes Distributed Active Archive Center (https://lpdaac.usgs.gov/). The spatial resolution of the T_s products (MOD11A1) is 1 km; however, the spatial resolution of T_s that we retrieved is 120 m. In order to correspond to the spatial resolution of the MOD11A1 T_s products, this paper calculated the mean T_s of the 8 × 8 pixels. The validation results are shown in Figure 3. The R^2 and RMSE are 0.74–0.85 and 2.5–2.9 K, respectively. This means that the results of estimated T_s are acceptable.

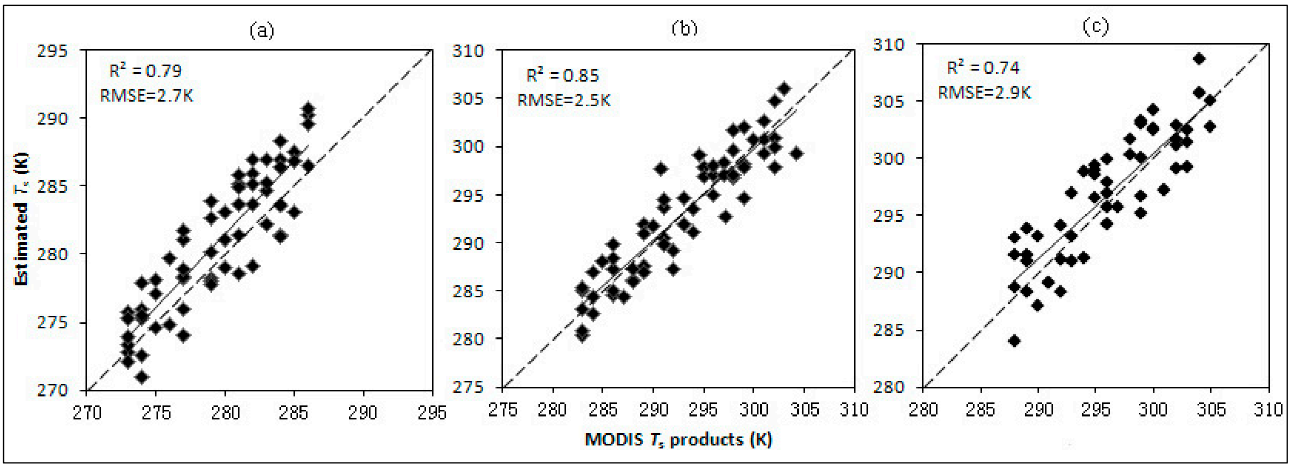

Figure 3. Comparison of the estimated T_s with the MODIS T_s products on: (**a**) 10 January 2011; (**b**) 18 May 2011; and (**c**) 23 September 2011.

3.5. Calculation of Temperature Vegetation Dryness Index

TVDI is a simplified land surface dryness index, which is based on an empirical formula of the relationship between T_s and NDVI, and only satellite-derived information is used in the method [10]. Therefore, the TVDI was used to estimate the soil moisture in the Laoshan forest. The scatter plots of the T_s/NDVI space often result in a trapezoidal shape [14,15]. Figure 4 shows the conceptual T_s/NDVI space.

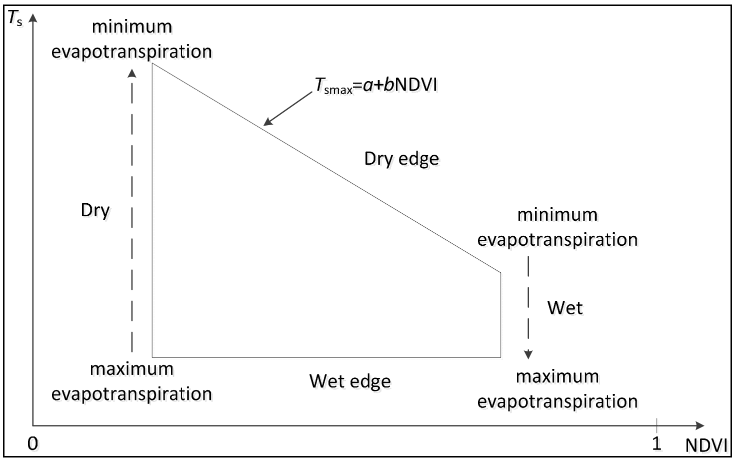

Figure 4. Definition of the TVDI. The TVDI for a given NDVI is estimated using T_s, T_{smin} and T_{smax} (see Equation (2)).

In the trapezium, the upper sloping edge of the trapezium is defined as the dry edge, and the lower sloping edge is defined as the wet edge; they represent extreme conditions of soil moisture and evapotranspiration. The points closer to the dry edge reflect a much stressed surfaces, with lower soil moisture in the root zone and higher T_s in the surface [17]. On the dry edge, as the NDVI increases along the x-axis, the maximum T_s decreases, and stomatal resistance to evapotranspiration is a key factor, which is partly controlled by the limited moisture availability [10]. On the other hand, the wet edge consists of a group of points forming a horizontal line. On the wet edge, under no-water-stress conditions, the T_s is independent of the NDVI. For the points closer to the wet edge, the evapotranspiration capacity and soil moisture become higher.

For a given pixel, T_{smax} are the values of T_s on the dry edge, respectively, for the value of the NDVI for that pixel. The TVDI is defined as [10]:

$$\text{TVDI} = (T_s - T_{smin})/(T_{smax} - T_{smin}) \quad (2)$$

and it can be determined on a pixel-by-pixel basis. On the dry edge, T_{smax} can be represented by straight line relations with the NDVI, *i.e.*, as:

$$T_{smax} = a + b(\text{NDVI}) \quad (3)$$

where the coefficients a and b can be determined by a least squares fit to the actual data.

In this paper, we used LANDSAT-5 TM images (Path 120, Row 32) for three different times of the year, 10 January 2011, 18 May 2011 and 23 September 2011, to determine the NDVI, T_s, T_{smin} and T_{smax} values.

4. Results and Discussion

4.1. Analysis of the T_s/NDVI Feature Space

The plots of T_{smin} and T_{smax} as a function of NDVI for the three scenes are shown in Figure 5. The peak values of the dry edge are in the bare soil. With the increase of NDVI values, the peak values of the dry edge reduce because of the high rate of evapotranspiration from vegetation canopies. The amount of annual average rainfall in Nanjing is 1090.6 mm; approximately 55% of the annual rainfall is between May and August. Therefore, the soil water is sufficient for evapotranspiration by vegetation canopies on 18 May 2011 and 23 September 2011, and T_{smin} decreases in line with NDVI increasing. There was precipitation on 17 September 2011, and the amount of rainfall was 16 mm; therefore, the slope of the dry edge and the wet edge on 23 September 2011 is greater than that on 18 May 2011. On 10 January 2011, T_{smin} increases slowly in line with NDVI increasing. The reason for this phenomenon is that the precipitation of Nanjing from the autumn of 2010 to the spring of 2011 was less than normal and caused continuous drought [31]. As a result, the soil water supply cannot fully meet the needs for vegetation evapotranspiration in the forest with vegetation cover increasing, and the slope of the dry edge on 10 January 2011 is less than that on 18 May 2011 and 23 September 2011.

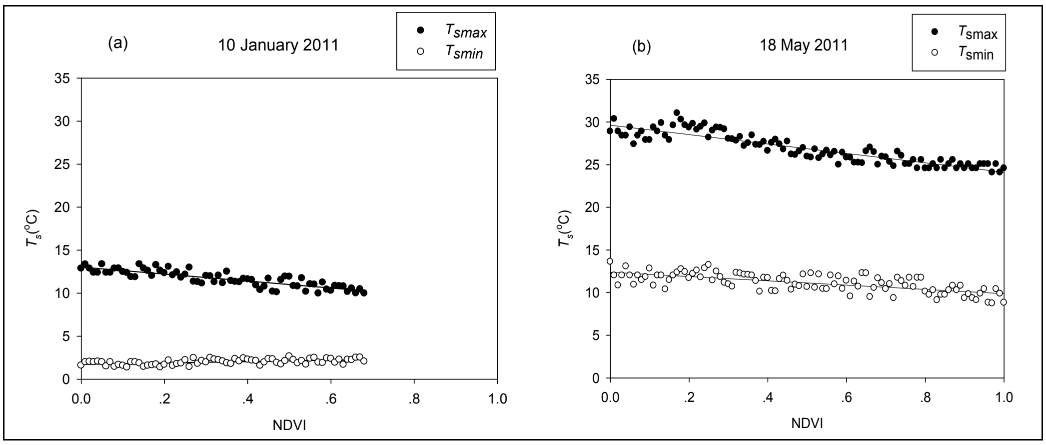

Figure 5. *Cont.*

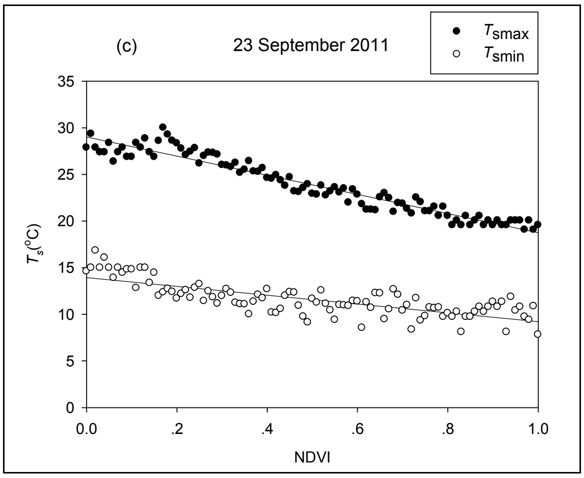

Figure 5. Plots of NDVI (x-axis) and surface temperature-T_s (y-axis) in the study. The maximum T_s and minimum T_s are extracted for small intervals (0.01) of NDVI.

Likewise, T_{smax} is negatively correlated with NDVI and can be obtained through linear regression. In order to determine the parameters describing the dry and wet edges, the maximum and minimum temperatures observed for small intervals of NDVI are extracted in the T_s/NDVI space. The values of the coefficients in Equation (3) for the dry edges and wet edges for the three scenes have been determined and are given in Table 2.

Table 2. Dry edges and wet edges in the T_s/NDVI space for the three scenes.

Date	Dry Edge	Wet Edge
10 January 2011	T_{smax} = –4.049 (NDVI) + 13.037 R^2 = 0.72	T_{smin} = 0.819 (NDVI) + 1.726 R^2 = 0.26
18 May 2011	T_{smax} = –5.510 (NDVI) + 29.621 R^2 = 0.82	T_{smin} = –2.514 (NDVI) + 12.387 R^2 = 0.46
23 September 2011	T_{smax} = –10.285 (NDVI) + 29.029 R^2 = 0.93	T_{smin} = –4.734(NDVI) + 13.942 R^2 = 0.59

4.2. Spatial Variation of TVDI

The TVDI of the Laoshan forest for the three different scenes has been calculated, and it is shown in Figure 6.

On 23 September 2011, there was a small amount of cloud in the sky. The region covered by cloud was screened out and is represented in black in Figure 6c. The area with low TVDI values on 23 September 2011 was larger than that on 18 May 2011. The mean of TVDI on 23 September 2011 was 0.56, and the mean of TVDI on 18 May 2011 was 0.60. However, the area with low TVDI values on 18 May 2011 was larger than that on 10 January 2011, and the mean of TVDI on 10 January 2011 was 0.74. The reason for this phenomenon is that the soil moisture is high between May and August in Nanjing, so the soil water is sufficient for evapotranspiration by vegetation canopies on 18 May 2011 and 23 September 2011. There was precipitation on 17 September 2011, so the TVDI on 23 September 2011 was lower than that on 18 May 2011. Because of the continuous drought from the autumn of 2010 to the spring of 2011, the TVDI on 10 January 2011 was higher than that on 23 September 2011 and 18 May 2011. There are some reservoirs in the Laoshan forest (see Figure 1), so the areas near the reservoirs have very low TVDI values, and the values are less than 0.5.

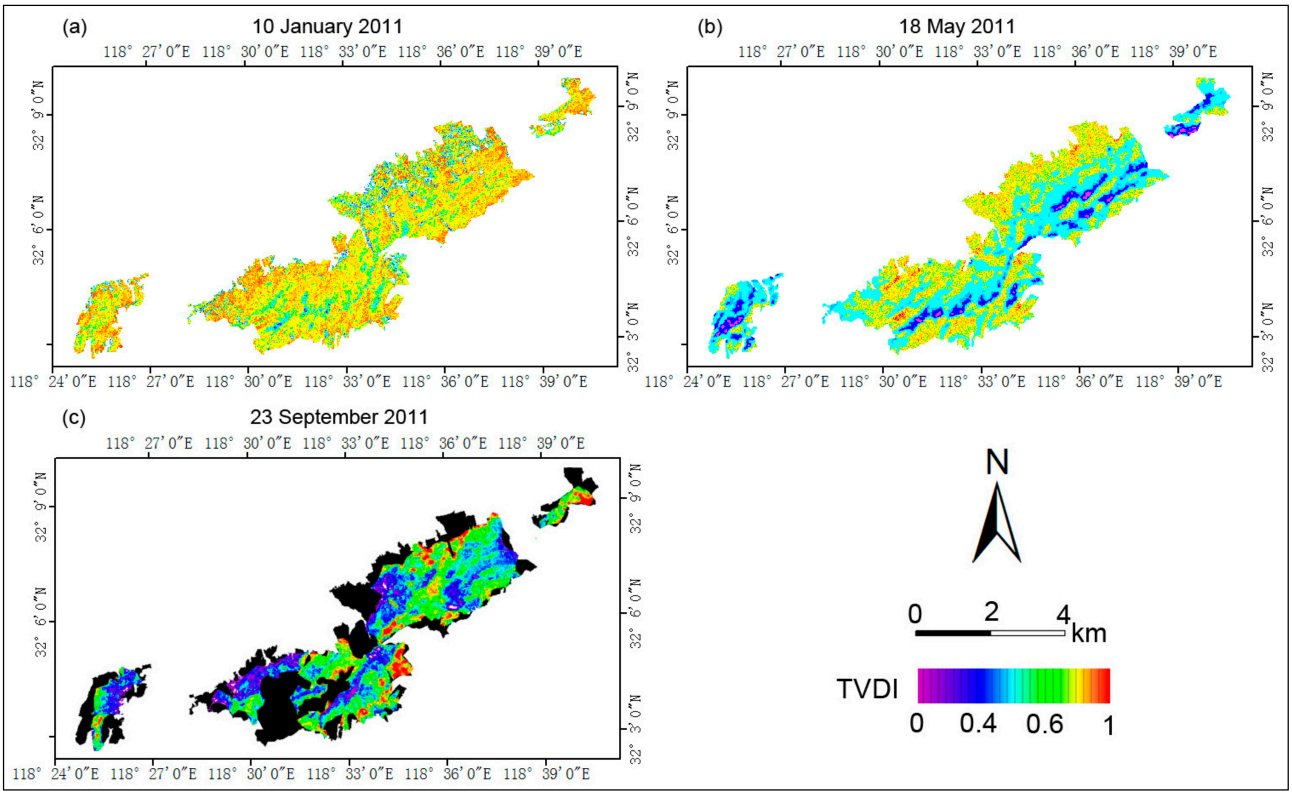

Figure 6. Spatial distribution of the TVDI for the three scenes. On 23 September 2011, the area covered by cloud was screened out and is represented in black in Figure 6c.

4.3. Comparison of TVDI with In Situ *Measurements*

The effectiveness of the TVDI as an index for assessing soil moisture was validated by systematically designed *in situ* soil moisture measurements for each land cover type (see Figure 1). Figure 7 shows the relationship between TVDI and the volumetric soil moisture at the observation points.

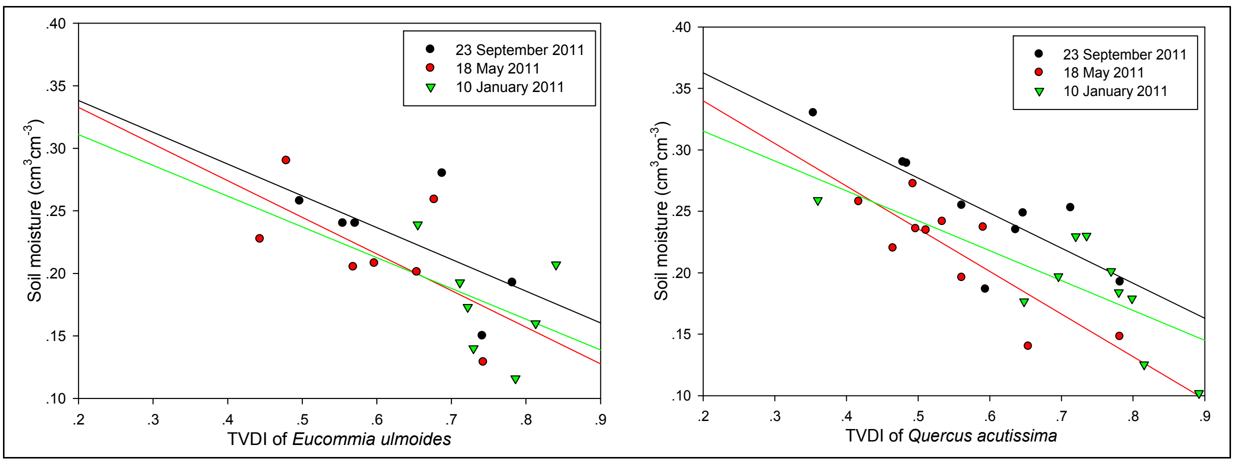

Figure 7. *Cont.*

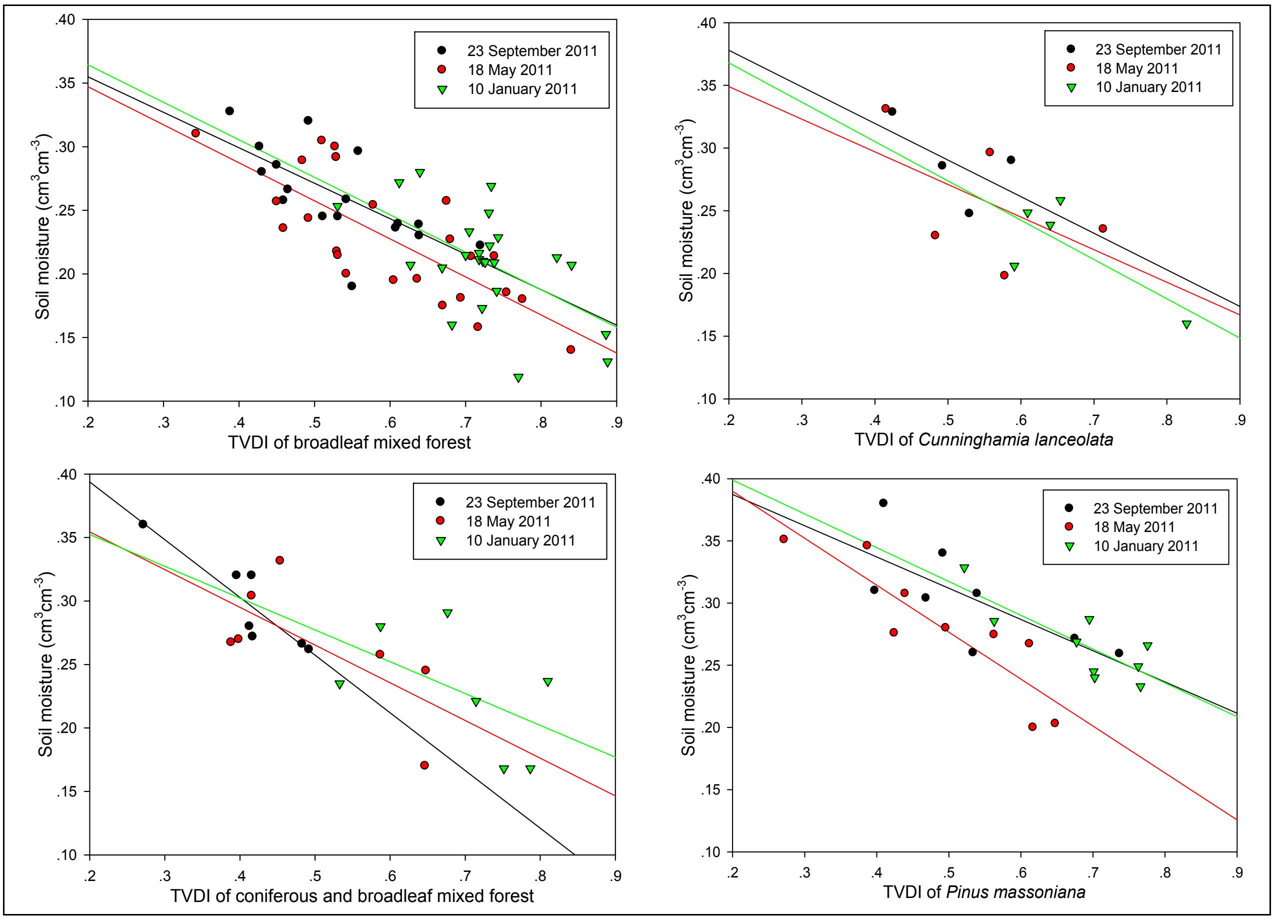

Figure 7. Comparison of the TVDI with the observation points of *in situ* soil moisture measurements for each land cover on 10 January 2011, 18 May 2011 and 23 September 2011.

On 23 September 2011, eleven observation points were of no use for validation purposes because of cloud, so only fifty-one observation points exist in Figure 7. Linear relationships exist between soil moisture and TVDI, and the coefficients in the equation of the regression line:

$$M_v = e(\text{TVDI}) + f \tag{4}$$

where M_v is the volumetric soil moisture, in cm^3/cm^3, the coefficients e and f can be determined by a least squares fit to the actual data and are given in Table 3 for the three different scenes that we have analyzed.

In Figure 7, soil moisture values plotted as a function of TVDI show higher TVDI values corresponding to lower soil moisture values. There is a significant negative correlation between the TVDI and the *in situ* measured soil moisture, and the standard errors of soil moisture estimation (SE) are low (SE = 0.015–0.041 cm^3/cm^3). Therefore, this means that the TVDI can reflect the soil moisture status. The relationships between soil moisture and TVDI are closer on 18 May 2011 and 23 September 2011 (R^2 = 0.29–0.8 and SE = 0.015–0.041 cm^3/cm^3) than on 10 January 2011 (R^2 = 0.15–0.65 and SE = 0.017–0.038 cm^3/cm^3). The poor correlation on 10 January 2011 is mainly due to the continuous drought from the autumn of 2010 to the spring of 2011 in Nanjing, and the sensitivity of the TVDI to soil moisture is lower under water-stressed surfaces, with lower soil moisture in the root zone. Thus, the plots are relatively scattered, and this is reflected in the rather low values of R^2. In the regions in which the land cover types are broadleaf mixed forest, *Quercus acutissima* and *Pinus massoniana*, the R^2 between the TVDI and soil moisture on 18 May 2011 (R^2 = 0.58–0.79) is higher than on 23 September 2011 (R^2 = 0.46–0.66). These regions occupied 89.1% of the area of the Laoshan forest. The reason for this phenomenon is that the values of NDVI on 23 September 2011 are higher than those on 18 May 2011 (see Figure 8). The mean of NDVI on 23 September 2011 is 0.61, and the mean of NDVI on 18 May 2011 is 0.54. This can reduce the sensitivity of the TVDI to soil moisture under high vegetation cover [7].

Table 3. The coefficients *e* and *f* of the regression equation (see Equation (4)) between the TVDI and soil moisture, standard errors of soil moisture estimation (SE) and R^2 values for linear fit of the data (units: cm^3/cm^3).

Date	Land Cover Type	*e*	*f*	R^2	SE
10 January 2011	*Eucommia ulmoides*	–0.25	0.36	0.15	0.036
	Quercus acutissima	–0.24	0.36	0.54	0.030
	broadleaf mixed forest	–0.29	0.42	0.34	0.033
	Cunninghamia lanceolata	–0.31	0.43	0.54	0.024
	coniferous and broadleaf mixed forest	–0.25	0.40	0.28	0.038
	Pinus massoniana	–0.27	0.45	0.65	0.017
18 May 2011	*Eucommia ulmoides*	–0.29	0.39	0.38	0.037
	Quercus acutissima	–0.35	0.41	0.68	0.024
	broadleaf mixed forest	–0.30	0.41	0.58	0.031
	Cunninghamia lanceolata	–0.26	0.40	0.29	0.041
	coniferous and broadleaf mixed forest	–0.30	0.41	0.47	0.034
	Pinus massoniana	–0.38	0.47	0.79	0.023
23 September 2011	*Eucommia ulmoides*	–0.25	0.39	0.38	0.034
	Quercus acutissima	–0.29	0.42	0.66	0.026
	broadleaf mixed forest	–0.28	0.41	0.46	0.026
	Cunninghamia lanceolata	–0.29	0.44	0.36	0.023
	coniferous and broadleaf mixed forest	–0.45	0.48	0.80	0.015
	Pinus massoniana	–0.25	0.44	0.53	0.027

Earlier studies used TVDI to estimate soil moisture from different remote sensing data and produced different R^2 values. These different remote sensing data are NOAA-AVHRR images (R^2 = 0.23–0.81) [10,16] and Terra/Aqua MODIS images (R^2 = 0.12–0.83) [7,8,17–20]. Gao *et al.* [21] used LANDSAT-5 TM images, but they did not calculate R^2 values. For some studies, the R^2 between the TVDI and soil moisture is still low [8,19]. The reason is that the TVDI values retrieved from remote sensing images suffer from scaling effects. For example, each pixel in the Landsat-5 TM image represents an area of 30 m × 30 m, but each observation point of *in situ* soil moisture measurement represents only a point on the soil surface, so the *in situ* measured soil moisture cannot ensure a perfect match with the corresponding pixel in the image.

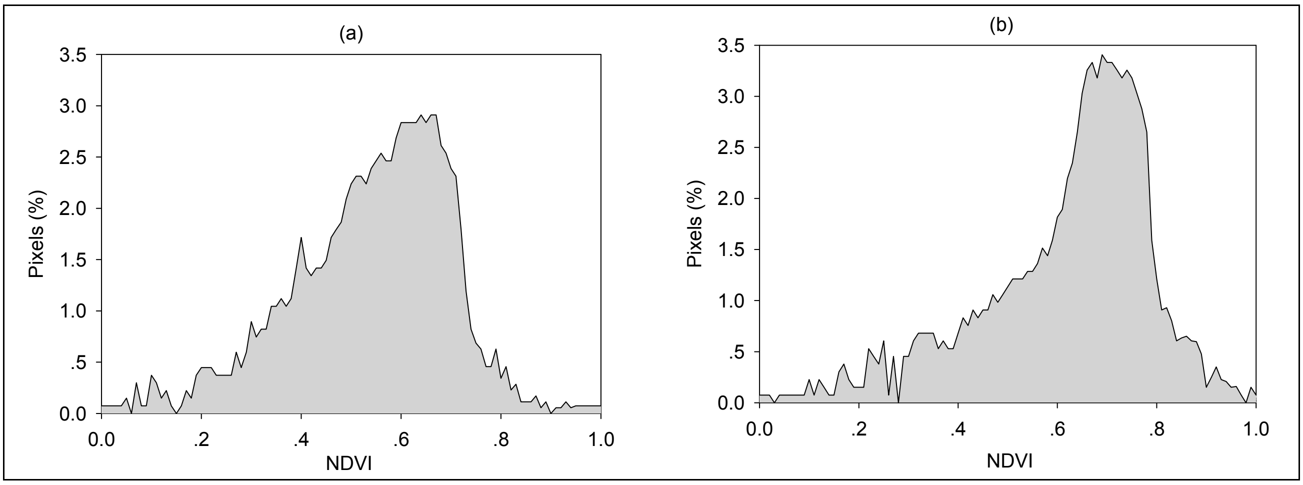

Figure 8. Histograms of the NDVI for (**a**) 18 May 2011 and (**b**) 23 September 2011.

4.4. Soil Moisture under Different Types of Land Cover

Table 3 shows that the standard errors of soil moisture estimation (SE) are low (SE = 0.015–0.041 cm^3/cm^3). Therefore, we have used the regression equation between the TVDI and soil moisture in Table 3 to calculate the soil moisture for the area associated with each type. Histograms for all six types are shown in Figure 9.

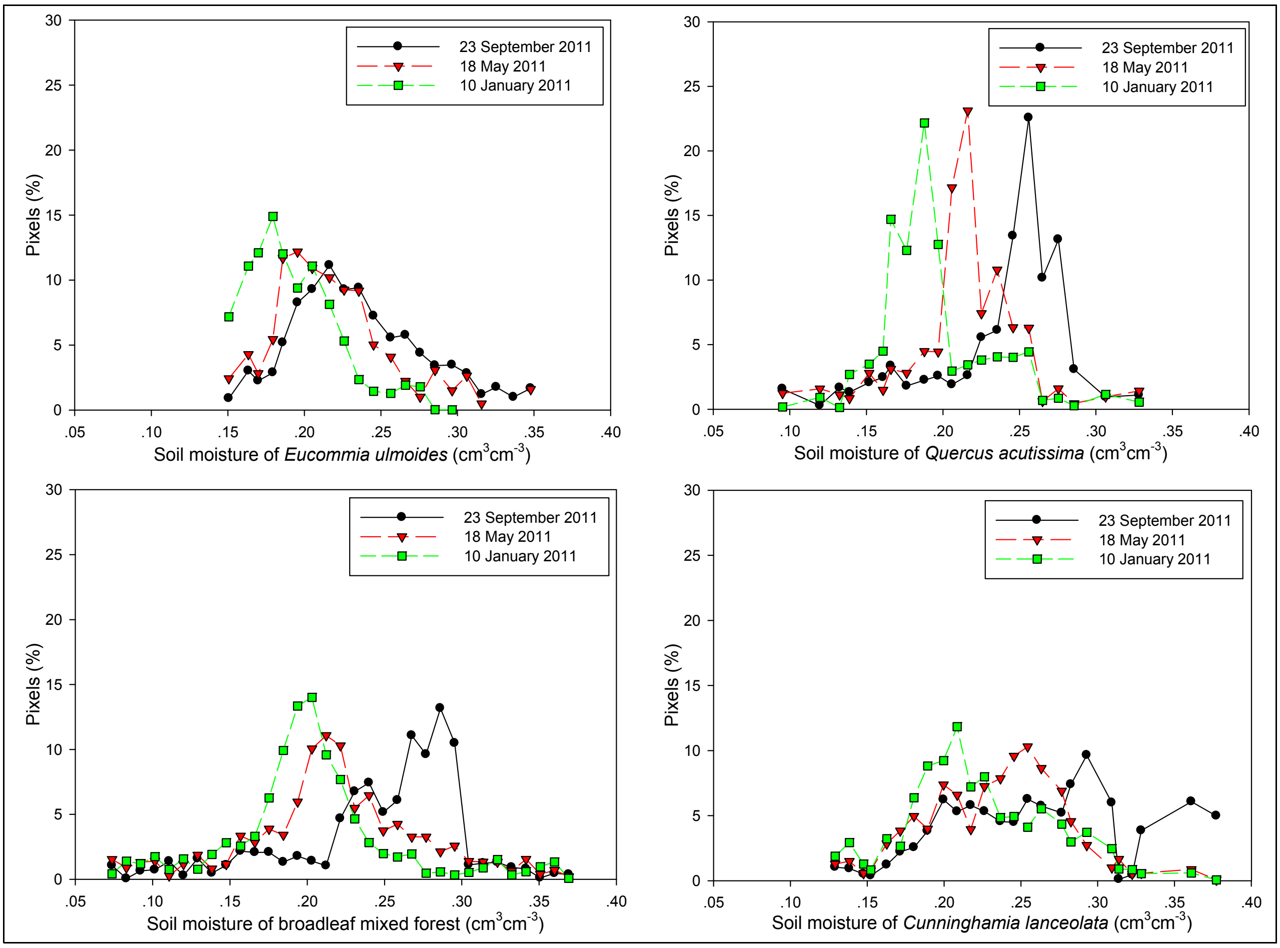

Figure 9. *Cont.*

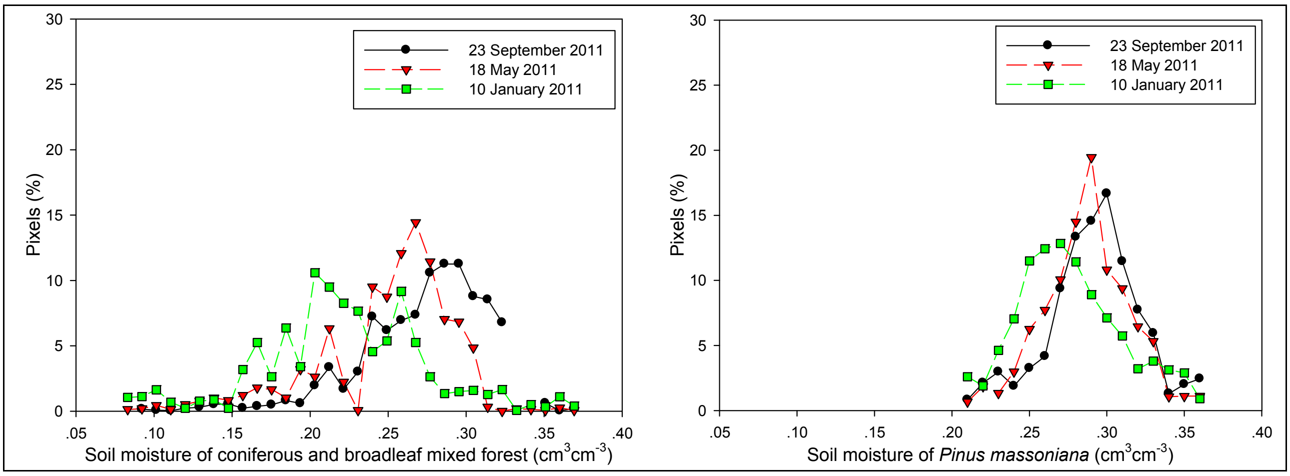

Figure 9. Histograms of the soil moisture under each type of land cover for the three scenes.

Figure 9 illustrates that the trends of soil moisture under each type of land cover for three different temporal patterns are similar to those of TVDI. The values of soil moisture on 23 September 2011 are higher than that on 18 May 2011, and the values of soil moisture on 18 May 2011 are higher than those on 10 January 2011. The mean values of soil moisture and variance under each type of land cover for the three scenes were calculated and are presented in Table 4.

Table 4 shows that the trends of soil moisture under the six types of land cover on 10 January 2011 are similar to those on 18 May 2011, and the mean values of soil moisture from low to high are listed in the following order: *Eucommia ulmoides*, *Quercus acutissima*, broadleaf mixed forest, *Cunninghamia lanceolata*, coniferous and broadleaf mixed forest and *Pinus massoniana*. However, on 23 September 2011, the mean value of soil moisture and variance under *Eucommia ulmoides* (mean = 0.2247, variance = 0.0014) is higher than that under *Quercus acutissima* (mean = 0.2198, variance = 0.0007). The reason for this phenomenon is that there was a small amount of cloud in the sky; although the region covered by cloud was screened out, the thin cloud also influences the accuracy of soil moisture estimation.

Table 4. The mean values of soil moisture and variance under each type of land cover for the three scenes (units: cm^3/cm^3).

Types	10 January 2011		18 May 2011		23 September 2011	
	Mean	**Variance**	**Mean**	**Variance**	**Mean**	**Variance**
Eucommia ulmoides	0.2072	0.0010	0.2149	0.0011	0.2247	0.0014
Quercus acutissima	0.2130	0.0004	0.2167	0.0009	0.2198	0.0007
broadleaf mixed forest	0.2154	0.0012	0.2360	0.0018	0.2448	0.0015
Cunninghamia lanceolata	0.2322	0.0017	0.2408	0.0014	0.2454	0.0012
coniferous and broadleaf mixed forest	0.2539	0.0032	0.2701	0.0022	0.2886	0.0016
Pinus massoniana	0.2745	0.0009	0.2869	0.0007	0.2917	0.0006

According to Table 4 and Figure 9, the soil water content under the six types of land cover from low to high is listed in the following order: *Eucommia ulmoides*, *Quercus acutissima*, broadleaf mixed forest, *Cunninghamia lanceolata*, coniferous and broadleaf mixed forest and *Pinus massoniana*.

5. Conclusions

The present study used LANDSAT-5 TM images to explore the potential of TVDI in the Laoshan forest. The relationship between TVDI and volumetric soil moisture at the observation points is significant. Furthermore, this paper investigates the ability of the TVDI to capture temporal variations in surface moisture. The results are encouraging and show that the TVDI values on 10 January 2011 are higher than those on 18 May 2011 and 23 September 2011 because of the continuous drought in the winter of 2011. The TVDI values after precipitation are lower than for periods of no precipitation. Therefore, it is summarized that the TVDI, which is solely based on satellite observations, is feasible for monitoring soil moisture in the Laoshan forest, and it can reflect the soil moisture status for three different times of the year.

Over the last decade, local government and scientists have raised many concerns about the hydrological roles of forests, and most studies use forest resource survey data and mathematical simulations to estimate the spatial variation of water holding of the forest ecosystems [32]. However, forest resource survey data and mathematical simulations need a lot of *in situ* measurements and are cost-intensive. So far, substantial research has been carried out to retrieve soil moisture using remotely-sensed observations [6], but little research focused on investigating the differences of soil moisture under different tree species. In this paper, an effort is also made to investigate the soil moisture under the six types of land cover via the TVDI with the aid of three different temporal patterns, and the soil moisture from low to high is listed in the following order: *Eucommia ulmoides*, *Quercus acutissima*, broadleaf mixed forest, *Cunninghamia lanceolata*, coniferous and broadleaf mixed forest and *Pinus massoniana*.

However, cloud cover seriously influences surface temperature retrieval and often limits the applicability of the TVDI for estimating soil moisture at a regional scale. The effects of scaling also have an impact on the accuracy of remotely-sensed soil moisture. Additional work using meteorological data and hydrological models, such as the soil water under forests (SWUF) model [33], should be done to test and validate the robustness of the TVDI over large regions.

Acknowledgments

This work was supported by the NSFC (National Natural Science Foundation of China) International Partnership Project under Grant Number: 3136113034; NSFC (National Natural Science Foundation of China) Project under Grant Number: 41171324; the Platform Project of Ministry of Science and Technology of China under Grant Number: 2005DKA32306; NSFC (National Natural Science Foundation of China) Project under Grant Number: 41101315; NSFC (National Natural Science Foundation of China) Project under Grant Number: 71373125; and JSNSF (Jiangsu Natural Science Foundation of China) Project under Grant Number: BK20140980.

Author Contributions

Shulin Chen and Zuomin Wen designed the sites of *in situ* measurements and built the modeling. Hong Jiang and Xiuying Zhang helped to perform the experiments and analyzed the data. Qinjian Zhao analyzed the accuracy and reliability of the method. Yan Chen participated in the editing of the paper.

Conflicts of Interest

The authors declare no conflict of interest.

References

1. Seneviratne, S.I.; Corti, T.; Davin, E.L.; Hirschi, M.; Jaeger, E.B.; Lehner, I.; Orlowsky, B.; Teuling, A.J. Investigating soil moisture—Climate interactions in a changing climate: A review. *Earth-Sci. Rev.* **2010**, *99*, 125–161.
2. Mathys, A.; Coops, N.C.; Waring, R.H. Soil water availability effects on the distribution of 20 tree species in western North America. *Forest Ecol. Manag.* **2014**, *313*, 144–152.
3. Wu, Y.M. Challenges and countermeasures of water resources in the process of urbanization. *Jiangsu Water Resour.* **2003**, *5*, 29–30. (In Chinese)
4. Skierucha, W.; Wilczek, A. A FDR sensor for measuring complex soil dielectric permittivity in the 10–500 MHz frequency range. *Sensors* **2010**, *10*, 3314–3329.
5. Skierucha, W.; Wilczek, A.; Szypłowska, A.; Sławiński, C.; Lamorski, K. A TDR-based soil moisture monitoring system with simultaneous measurement of soil temperature and electrical conductivity. *Sensors* **2012**, *12*, 13545–13566.
6. Grayson, R.B.; Western, A.W. Towards areal estimation of soil water content from point measurement: Time and space stability of mean response. *J. Hydrol.* **1998**, *207*, 68–82.
7. Patel, N.R.; Anapashsha, R.; Kumar, S.; Saha, S.K.; Dadhwal, V.K. Assessing potential of MODIS derived temperature/vegetation condition index (TVDI) to infer soil moisture status. *Int. J. Remote Sens.* **2009**, *30*, 23–39.
8. Chen, S.L.; Liu, Y.B.; Wen, Z.M. Satellite retrieval of soil moisture: An overview. *Adv. Earth Sci.* **2012**, *27*, 1192–1203. (In Chinese)
9. Goetz, S.J. Multi-sensor analysis of NDVI, surface temperature and biophysical variables at a mixed grassland site. *Int. J. Remote Sens.* **1997**, *18*, 71–94.
10. Sandholt, I.; Rasmussen, K.; Andersen, J. A simple interpretation of the surface temperature vegetation index space for assessment of surface moisture status. *Remote Sens. Environ.* **2002**, *79*, 213–224.
11. Goward, S.N.; Xue, Y.K.; Czajkowski, K.P. Evaluating land surface moisture conditions from the remotely sensed temperature/vegetation index measurements: An exploration with the simplified simple biosphere model. *Remote Sens. Environ.* **2002**, *79*, 225–242.
12. Friedl, M.A.; Davis, F.W. Sources of variation in radiometric surface temperature over a tallgrass prairie. *Remote Sens. Environ.* **1994**, *48*, 1–17.
13. Carlson, T.N.; Gillies, R.R.; Perry, E.M. A method to make use of thermal infrared temperature and NDVI measurements to infer surface soil water content and fractional vegetation cover. *Remote Sens.* **1994**, *9*, 161–173.
14. Moran, M.S.; Clarke, T.R.; Inoue, Y.; Vidal, A. Estimating crop water deficit using the relation between surface–Air temperature and spectral vegetation index. *Remote Sens. Environ.* **1994**, *49*, 246–263.

15. Xin, J.F.; Tian, G.L.; Liu, Q.H.; Chen, L.F. Combining vegetation index and remotely sensed temperature for estimation of soil moisture in China. *Int. J. Remote Sens.* **2006**, *27*, 2071–2075.
16. Wang, C.Y.; Qi, S.H.; Niu, Z.; Wang, J.B. Evaluating soil moisture status in China using the temperature–vegetation dryness index (TVDI). *Can. J. Remote Sens.* **2004**, *30*, 671–679.
17. Holzman, M.E.; Rivas, R.; Piccolo, M.C. Estimating soil moisture and the relationship with crop yield using surface temperature and vegetation index. *Int. J. Appl. Earth Obs.* **2014**, *28*, 181–192.
18. Zhang, F.; Zhang, L.W.; Shi, J.J.; Huang, J.F. Soil moisture monitoring based on land surface temperature—vegetation index space derived from MODIS data. *Pedosphere* **2014**, *24*, 450–460.
19. Chen, J.; Wang, C.Z.; Jiang, H.; Mao, L.X.; Yu, Z.R. Estimating soil moisture using Temperature—Vegetation Dryness Index (TVDI) in the Huanghuai-hai (HHH) plain. *Int. J. Remote Sens.* **2011**, *32*, 1165–1177.
20. Rahimzadeh-bajgiran, P.; Omasa, K.; Shimizu, Y. Comparative evaluation of the Vegetation Dryness Index (VDI), the Temperature Vegetation Dryness Index (TVDI) and the improved TVDI (iTVDI) for water stress detection in semi-arid regions of Iran. *ISPRS J. Photogramm.* **2012**, *68*, 1–12.
21. Gao, Z.Q.; Gao, W.; Chang, N.B. Integrating temperature vegetation dryness index (TVDI) and regional water stress index (RWSI) for drought assessment with the aid of LANDSAT TM/ETM+ images. *Int. J. Appl. Earth Obs.* **2011**, *13*, 495–503.
22. Luan, H.J.; Tian, Q.J.; Yu, T.; Hu, X.L.; Huang, Y.; Du, L.T.; Zhao, L.M.; Wen, X.; Han, J.; Zhang Z.W.; *et al*. Modeling continuous scaling of NDVI based on fractal theory. *Spectrosc. Spect. Anal.* **2013**, *33*, 1857–1862. (In Chinese)
23. Sun, L.; Sun, R.; Li, X.; Liang, S.; Zhang, R. Monitoring surface soil moisture status based on remotely sensed surface temperature and vegetation index information. *Agr. Forest Meteorol.* **2012**, *166*, 175–187.
24. Mallick, K.; Bhattacharya, B.K.; Patel, N.K. Estimating volumetric surface moisture content for cropped soils using a soil wetness index based on surface temperature and NDVI. *Agr. Forest Meteorol.* **2009**, *149*, 1327–1342.
25. Chander, G.; Markham, B.L.; Helder, D.L. Summary of current radiometric calibration coefficients for Landsat MSS, TM, ETM+, and EO-1 ALI sensors. *Remote Sens. Environ.* **2009**, *113*, 893–903.
26. French, A.N.; Norman, J.M.; Anderson, M.C. A simple and fast atmospheric correction for spaceborne remote sensing of surface temperature. *Remote Sens. Environ.* **2003**, *87*, 326–333.
27. Qin, Z.; Karnieli, A.; Berliner, P. A mono-window algorithm for retrieving land surface temperature from Landsat TM data and its application to the Israel-Egypt border region. *Int. J. Remote Sens.* **2001**, *22*, 3719–3746.
28. Sobrino, J.A.; Jiménez-muñoz, J.C.; Paolini, L. Land surface temperature retrieval from LANDSAT TM 5. *Remote Sens. Environ.* **2004**, *90*, 434–440.
29. Xiao, R.B.; Weng, Q.H.; Ouyang, Z.Y.; Li, W.F.; Schienke, E.W.; Zhang, Z.M. Land surface temperature variation and major factors in beijing, China. *Photogramm. Eng. Rem. S.* **2008**, *74*, 451–461.

30. Wang, F.; Qin, Z.H.; Song, C.Y.; Tu, L.L.; Karnieli, A.; Zhao, S.H. An improved mono-window algorithm for land surface temperature retrieval from landsat 8 thermal infrared sensor data. *Remote Sens.* **2015**, *7*, 4268–4289.
31. Duan, Y.; Wang, W.; Cai, X.J. Applied analyses on Palmer, SPEI and CI Indices of drought process in Yangtze-Huaihe River Basins during winter of 2010/spring of 2011. *Plateau Meteorol.* **2013**, *32*, 1126–1139. (In Chinese)
32. Pollacco, J.A.P. A generally applicable pedotransfer function that estimates field capacity and permanent wilting point from soil texture and bulk density. *Can. J. Soil Sci.* **2008**, *88*, 761–774.
33. Paul, K.I.; Polglase, P.J.; O'Connell, A.M.; Carlyle, J.C.; Smethurst, P.J.; Khanna, P.K.; Worledge, D. Soil water under forests (SWUF): A model of water flow and soil water content under a range of forest types. *Forest Ecol. Manag.* **2003**, *182*, 195–211.